

Loran-C User Position Software (LUPS) Navigation Performance with PC-104 and DDC Receiver Flight Test Data in the New Jersey Area

Jaime Y. Cruz, Robert Stoeckly, Robert W. Lilley, John G. Kirk, Steven Chavin
Illgen Simulation Technologies, Inc. (ISTI)
jcruz@illgen.com, rstoeckly@illgen.com

ABSTRACT

The Loran-C User Position Software (LUPS) developed by ISTI was used to post-process PC-104 and DDC receiver data collected during the Federal Aviation Administration Technical Center (FAATC) 19 – 22 June 2001 flight tests along the New Jersey to North Carolina coastal areas. This paper summarizes the special features of LUPS and reports the achieved navigation performance in terms of accuracy, integrity, continuity, and availability metrics. The results show a 95% accuracy of about 470 meters using the PC-104 and 320 meters using the DDC data relative to truth GPS horizontal positions. The difference is attributed mainly to the lower average number of signals available in the PC-104 compared to the DDC data (5.3 versus 7.6). For a total of 7.9 hours of normal receiver operation, the results show no integrity failures in terms of Hazardously Misleading Information, less than 0.03% Misleading Information, better than 99.9% continuity in terms of the number of alarms raised, and better than 99.9% availability of (formal) accuracy and integrity. Processing of more flight test data in various geographic areas is recommended to increase the statistical confidence in these results and to effect system improvements. More work needs to be done on the validation/calibration of the Fault Detection and Exclusion (FDE), as opposed to fault-free, protection levels.

1. INTRODUCTION

LUPS is an all-in-view, weighted least squares Loran-C navigation software package which includes a propagation delay model based on the FCC M3 ground conductivity database, measurement fault detection and exclusion, propagation delay spatial-error covariance modeling, and propagation/ emission delay temporal-variation covariance modeling. The algorithms implemented in LUPS are detailed in [1]. This paper summarizes the relevant algorithms and presents the results of using LUPS to post-process Loran-C receiver data from the 19 – 22 June 2001 flight tests conducted by the FAATC. The data used were from the PC-104 and DDC receivers developed by the United States Coast Guard Academy (USCGA).

2. LUPS SPECIAL FEATURES

Weighted Least Squares Estimation

An iterative, weighted, least squares navigation solution is computed based on the observation residuals, and with the weight matrix being the inverse of the covariance matrix of observation residuals. The observation residuals are the differences between measured and modeled Time-of-Arrival (TOA) values. The modeled TOAs are computed based on the resolved inter-chain timing

ambiguities, published emission delays, computed propagation delays, and the geometric ranges and receiver clock offset from the current navigation estimates. The software provides estimates for the receiver latitude, longitude, and clock offset, and the statistical position error and protection level.

The covariance matrix of observation residuals is computed as the sum of the TOA error covariance matrix, propagation delay spatial-error covariance matrix, and propagation/emission delay temporal-variation covariance matrix, with the sum multiplied by the reference variance. The TOA error covariance matrix is computed based on the measured signal-to-noise ratios (SNR) of the TOA measurements and on the configurable standard deviations of Master-clock-to-UTC synchronization error, Secondary-to-Master clock synchronization error, and lumped contributions from other error sources. The propagation delay spatial-error covariance and propagation/emission delay temporal-variation covariance models are described below. The reference variance provides a global scaling of all covariances, and is used for offline tuning of the covariances against observed residuals.

Propagation Delay Model

The Loran signal propagation delay along a given path is calculated using the Millington-Pressley

algorithm for phase [2, 3], based on the path conductivity profile extracted from an edited version of the FCC M3 ground conductivity database [4]. The propagation delay for each uniform-conductivity section of the step-function profile is computed using Brunavs' formula [5], in which the delay is expressed in terms of the path length and five constant coefficients. The Brunavs coefficients are tabulated for specific conductivities, and the delay corresponding to the input conductivity is found by interpolation from two delays computed from the tabulated values. The computed delay includes the effects of the Loran-C primary, secondary, and additional secondary factors.

Fault Detection and Exclusion (FDE)

Student's t-test is applied to detect unexpectedly large observation residuals based on a comparison of each residual with its formal standard deviation ([6] Section 5). Large residuals are flagged for exclusion from the least squares navigation estimation. The t-test is conducted at a significance level of 0.001. The FDE protection level is also computed with assumed probabilities of 10^{-3} for missed detection and 10^{-6} for false alarm ([6] Section 7 and Figure 9 discussion).

Propagation Delay Spatial-Error Covariance Model

The propagation delay error covariance matrix among the propagation paths being used in the navigation is intended to represent modeling errors due to spatial errors in the ground conductivity database. The covariance is computed for each pair of receiver-to-transmitter paths as a double line integral (along the two paths) of a postulated scale-factor error covariance function. The scale-factor error covariance is a function of the distance between the two points being correlated, and is assumed to be homogeneous (location independent) and isotropic (azimuth independent) throughout the operating area. The covariance function is parameterized by the variance, which is the value at zero distance, and the correlation length, which is the distance at which the covariance drops to half the variance. Detailed definitions and formulas are given in [7] Sections 3 and 4.1.

Propagation/Emission Delay Temporal-Variation Covariance Model

The propagation/emission delay variation covariance matrix among the propagation paths being used in the navigation is intended to represent modeling errors due to temporal variations in the propagation/emission delay. The temporal variations may be due to seasonal, weather, and diurnal effects. The covariance for each pair of receiver-to-transmitter paths is computed as the sum of double line integrals (along the receiver-to-transmitter, SAM-to-Master, and SAM-to-Secondary paths) of a postulated scale-factor error covariance function. The scale-factor error covariance function is of the same form as that used with the spatial-error covariance model, but with a separate set of covariance parameters. The integral formulas are given in [7] Sections 4.1 to 4.3.

Inter-Chain Timing Ambiguity Resolution

The clock offset parameter being estimated in the LUPS navigation solution is the Time-of-Emission (TOE) of the base chain as measured by the receiver's clock. The base chain is chosen to be the chain with the strongest signals received. In order to model the signals from chains other than the base chain, the phase relationships of the chains with respect to the base chain must be resolved. This is accomplished in LUPS by performing a preliminary weighted least squares solution, called the cross-chain solution, which is the same as the main navigation estimation except that the unknowns are the receiver latitude and longitude, plus one time parameter (the TOE_i) for each chain i being used. Each estimated TOE_i is then rounded off to the nearest multiple n_i of the configurable parameter Δ relative to the estimated TOE of the base chain. For the North American chains, the parameter Δ is normally configured to 100 μ s (the greatest common factor of all GRIs) for the SatMate receiver and to 200 μ s (GCF of all PCIs) for the USCGA's PC-104 and DDC receivers. The resolved timing ambiguities $n_i\Delta$ are then used in modeling the TOAs for the main navigation estimation.

FCC M3 Conductivity Database Editing

In reformatting the FCC M3 ground conductivity file to create the LUPS database, some editing was also performed. The list below records all additions, deletions, and modifications made to the original FCC M3 data. The conductivity cells are bounded by "edges."

- Elimination of zero-length edge - One edge with zero length was found and eliminated from the database.
 - Correction of edge locations – Twelve pairs of edges, which did not close their corresponding cells exactly, were corrected by moving one edge of each pair.
 - Correction of conductivity values – As one proceeds counterclockwise along the boundary of a conductivity cell, the conductivity to the left of each edge should be the same. Six conductivity values did not satisfy this requirement and were corrected.
 - Outer boundary of the database coverage area – The FCC M3 database covers most of North America but excludes Alaska, the far northern islands of Canada, Greenland, and Central America. The safest treatment of the outer boundary would be to draw a boundary extending far out into the ocean. The conductivity beyond this boundary would be considered unknown, and any groundwave path extending beyond the boundary would be discarded.
- The current version of LUPS uses a simpler treatment for the database. The outer boundary mostly follows the coastline of the North American mainland and crosses land only along the Alaska/Canada border and along the southern border of Mexico. The conductivity beyond this boundary is that of seawater, and there is no limit on the length of a groundwave path. The main disadvantage of this treatment is that paths across Alaska are treated incorrectly and are not discarded.
- Addition of edges to treat “island” cells – This deals with a cell or group of cells that is surrounded by a single cell. The coverage of the surrounding cell must exclude that of the “island” cell or cells. For this purpose, a pair of oppositely directed edges is added between a vertex of the “island” and a nearby vertex of the surrounding cell. The boundary of the surrounding cell goes counterclockwise around its outer boundary, across the cell to the “island”, clockwise around the island, and back across the cell to its outer boundary. Eighteen “island” cells were treated in this manner.
 - Cells with uncertain conductivity – The FCC M3 dataset contains conductivity values of 101, 102, 110, 120, and 199 mS/m. These

unrealistic values, appearing in sparsely populated areas of Canada, were changed to values that seem more reasonable.

3. FLIGHT TEST RESULTS

LUPS Configuration Parameters

The values of the LUPS configuration parameters used in this report are shown in Table 1, unless otherwise stated in the table or plot of results. The parameters of the TOA error covariance, propagation delay spatial-error covariance, and propagation/emission delay temporal-variation covariance models were those resulting from the LUPS integration tests [1] with PC-104 and SatMate data. Only receiver measurements with Envelope-to-Cycle Difference (ECD) between -10 and 10 μ sec and SNR greater than -10 dB (for the PC-104) and -15 dB (for the DDC) were considered for use in the LUPS navigation solution.

Figure 1 helps visualize the propagation delay standard error implied by the scale-factor error covariance parameters given in Table 1.

Flight Paths

Figures 2 to 5 show the flight paths for the 19 to 22 June 2001 tests, respectively. The gaps in the plot correspond to drop outs of the PC-104 (19 to 21 June) and DDC (22 June) receiver-generated position solutions.

Truth GPS Positions

The truth GPS positions consisted of Ashtech differential GPS solutions received with the Loran-C receiver files. The Loran-C receiver time tags were slaved to the GPS 1-PPS signals. The value 13 seconds, the number of leap seconds accounting for the current difference between GPS time and UTC, was subtracted from the time tags of the GPS truth data in order to align with the UTC time tags of the Loran receiver data.

Horizontal Navigation Errors

Figures 6 to 9 show the horizontal navigation errors of the receiver-generated and LUPS solutions, for the 19 to 22 June 2001 tests, respectively. Only receiver-generated solutions flagged as “good fixes” by the receiver are plotted. The 0.25-n.mi. accuracy threshold is also plotted

for reference. The results show three periods of abnormal PC-104 receiver operation at 324072 – 324870, 327450 – 327930, and 398976 – 403221 seconds UTC, and one period of abnormal DDC operation at 486400 – 487000 seconds UTC.

During periods of normal receiver operation the LUPS errors are generally below the 0.25-n.mi. threshold while the receiver-native errors are above the threshold. This significant improvement is due to the use of the ground-conductivity based propagation delay model in LUPS (see the test in Figure 11).

Also, during normal receiver operation, solution spikes that occur in the receiver-native solution do not occur in the LUPS solution (see Figure 9). This is due to the use of measurement fault detection and exclusion (FDE) in LUPS.

Number of Signals Used

Figure 10 compares the number of signals used in the DDC-generated versus LUPS-generated solution for the 22 June data. The differences are due to the use of FDE in LUPS and possible differences in measurement reasonability criteria (LUPS used ECD and SNR tolerances). The average number of signals used is 7.5 in the DDC-native and 7.6 in the LUPS solution. For the 19 – 21 June data (not plotted) the average number of signals used is lower, equal to 5.7 for the PC-104-native and 5.3 for the LUPS solution.

The PC-104 and DDC receivers can receive signals from up to three chains. Since different chains were selected for the DDC receiver on 22 June and for the PC-104 on 19 – 21 June (see Table 1), the number of signals from the DDC and PC-104 receivers are not comparable.

Effect of Ground Conductivity Model

Figure 11 shows the dramatic improvement in accuracy when using the ground conductivity based propagation delay model (Figure 9) versus the simpler all-seawater conductivity model. The several-hundred-meter accuracy improvement causes the navigation accuracy requirement to be met.

Some Parameter Tuning

Figure 12 shows the significance of applying a proper set of signal reasonability criteria before the FDE. When the SNR tolerance for the DDC data

was reduced from -15 to -20 dB, spikes showed up in the LUPS solution (compare Figures 9 and 12). The generic reason for the spikes was that one bad signal or another pulled the solution such that the FDE excluded not only the bad signal but also one good signal (Seneca 9960M). The good signal happened to be very important to the geometry of the solution, and without that signal the solution produced the observed spikes.

Figure 13 shows the horizontal errors when using the 22 June DDC data, after some tuning of the error parameters to account for the observed better performance with the DDC compared to the PC-104 data. Previous tuning during the LUPS integration tests had used PC-104 and SatMate data only. The standard deviation was reduced from 50 m to 20 m at 0 dB SNR for the TOA noise, and from 110 m to 60 m for “other error sources,” compared to the baseline case. The “other” error sources include cross-wave interference, cross-rate interference, and skywave contamination. The resulting navigation errors look very similar to those in the baseline case (compare Figures 9 and 13). The significant impact is on the formal error estimates, as discussed with Figure 17 below.

East and North Navigation Errors

Figure 14 shows the receiver-native and LUPS east and north navigation errors using the 19 – 21 June PC-104 data (left plot) and 22 June DDC data (right plot). The 0.25-n.mi. accuracy threshold is also plotted for reference. The reduced bias and scatter of the LUPS solution compared to the receiver-native solution is evident. The achieved improvement is attributed to the use of the conductivity-based propagation delay model and measurement fault detection and exclusion in LUPS.

Figure 15 shows the east and north errors when using DDC-tuned error parameters in LUPS, and either including (left plot) or excluding (right plot) the results for the period of abnormal receiver operation. The improvement relative to the baseline case (Figure 14, right plot) is noticeable but not dramatic. The dramatic improvement is in the formal error estimates, as discussed with Figure 17 below.

Achieved Accuracy Performance

Accuracy performance is assessed by the statistics of truth horizontal navigation errors. Specifically,

the 95% error value (i.e., 95% of all errors are less than or equal to this value) is to be compared with the assumed 2-sigma accuracy requirement of 0.25 n.mi. (463 meters).

Table 2 shows the statistics of LUPS navigation errors with the 19 – 21 June PC-104 and 22 June DDC receiver data. The statistics for 22 June reflect the use of DDC-tuned error parameters (Figure 15, left plot). The 95% error value for PC-104 data is 469 m, which is marginal. The 95% and 99.9% errors using DDC data are 322 and 399 m, respectively, which exceed the accuracy requirement. The difference in accuracy between the PC-104 and DDC data is attributable to the lower average number of signals available in the PC-104 compared to the DDC data (5.3 versus 7.6).

Integrity/Continuity/Availability Performance Diagram

A performance diagram, analogous to that used by Stanford University [8], is used to depict the integrity, continuity, and availability of the LUPS navigation solution. The diagram is a scatter plot of horizontal error versus fault-free horizontal protection level (FFHPL). The FFHPL represents an error bound with the assumption that the errors obey the Normal probability distribution. FFHPL is taken here to be equal to six times the semimajor axis of the error ellipse. Three lines are drawn to divide up the (error, FFHPL) space into four regions as follows (see Figure 16 for example):

- **System Unavailable** – This region is defined by the condition: $2 \times \text{semimajor axis} > 463 \text{ m}$.

Note: Availability here means availability of both accuracy and integrity. Accuracy is available if the 95% accuracy probability level (taken as 2 times the semimajor axis of the error ellipse) is less than or equal to the accuracy requirement of 463 m. Integrity is available if the FFHPL (taken as 6 times the semimajor axis of the error ellipse) is less than or equal to the horizontal alert limit (HAL). HAL is taken here to be 1 n.mi (1852 m). Hence, availability is driven by the accuracy requirement since $2 \times \text{semimajor axis} \leq 463 \text{ m}$ automatically implies $\text{FFHPL} \leq \text{HAL}$.

- **Hazardously Misleading Information (HMI)** – This region corresponds to the case when the system is available and the error is greater than the alert limit, i.e., the conditions: $2 \times \text{semimajor axis} \leq 463 \text{ m}$ and $\text{Error} > \text{HAL}$.

- **Misleading Information (MI)** – This region is defined by the conditions: $2 \times \text{semimajor axis} \leq 463 \text{ m}$, $\text{Error} \leq \text{HAL}$, and $\text{Error} > \text{FFHPL}$.
- **Normal Operation** – This region is defined by the conditions: $2 \times \text{semimajor axis} \leq 463 \text{ m}$ and $\text{Error} \leq \text{FFHPL}$.

To quantify performance, the number of test epochs falling inside the MI and HMI regions, and the number and percentage of epochs in the System Unavailable region, are indicated in the diagram. Currently, we quantify continuity by the number of alarms raised, where an alarm is defined as a transition from the System Available to System Unavailable state.

The performance goal is to have very high system availability (low formal errors) while having no HMI, little or no MI cases, and very high continuity (low number of alarms). Availability is an economic attribute of the system, while accuracy, integrity, and continuity are safety attributes.

Achieved Integrity, Continuity, and Availability Performance

Figure 16 shows the initial LUPS navigation performance diagrams for the 19 – 21 June PC-104 (left plot) and 22 June DDC (right plot) receiver data. The plots include the epochs of abnormal receiver operation noted earlier. Improvements to these initial results are given next.

Figure 17 shows improved LUPS performance with the 22 June DDC data after using DDC-tuned error parameters and either including (left plot) or excluding (right plot) the epochs of abnormal receiver operation at 486400 – 487000 seconds UTC. Figure 18 shows improved performance with the 19 – 21 June PC-104 data after excluding the three periods of abnormal receiver operation.

These results are encouraging. During normal receiver operation there is no HMI, less than 0.03% MI, better than 99.9% continuity considering the number of alarms, and better than 99.9% availability (of accuracy and integrity).

Achieved FDE Protection Levels

Strictly, epochs for which the FDE protection level exceeds the assumed alarm limit of 1852 meters must also belong to the “System Unavailable”

category. If this condition is applied, the availability reduces dramatically to 7.7% for the 19 – 21 June data and 57.3% for the 22 June data. The driver for this is the number of signals used in the navigation. With the current tuning of the FDE protection level computations (assumed probabilities of 10^{-3} for missed detection and 10^{-6} for false alarm; see [6] Figure 2) and the error models, a minimum of about 8 signals in good geometry is needed for availability of the FDE function. More validation and calibration work is needed in this area.

4. CONCLUSIONS/RECOMMENDATIONS

The results indicate that all-in-view Loran-C can meet the required navigation performance provided that a ground-conductivity based propagation delay model, measurement fault detection and exclusion, and properly calibrated error models are used in the weighted least squares estimation. This conclusion is based on only 5.3 hours worth of PC-104 and 2.6 hours worth of DDC flight test data along the New Jersey to North Carolina coastal areas. Processing of more flight test data in various geographic areas is recommended in order to increase statistical confidence in the results and to effect improvements. Specific improvements can be made to the conductivity database, calibration of receiver and propagation-path error models, and signal reasonability criteria.

Future plans for LUPS include the conversion to a real-time receiver-integrated version, and the extension to a hybrid GPS/Loran-C software. Additionally, more work needs to be done on the validation and calibration of the FDE protection level (as opposed to the FFHPL).

REFERENCES

- [1] "Loran-C User Position Software (LUPS) Engineering Notes Version 1.0," Illgen Simulation Technologies, Inc., IST2001-R-247, 25 May 2001.
- [2] "Ground-wave Propagation over an Inhomogeneous Smooth Earth," Millington, G., Proc. IEE, Volume 96, Part III, No. 39, 1949, pp. 53-64.
- [3] "The Measurement of the Phase Velocity of Ground-wave Propagation at Low Frequencies over a Land Path," Pressey, B.G., G.E. Ashwell, and C.S. Fowler, Proc. IEE, Volume 100, Part III, No. 64, 1953, pp. 73-84.

- [4] FCC M3 Map Data File, Federal Communications Commission, PB81-211567, 1981 (available from the National Technical Information Service).

- [5] "Phase Lags of the 100 kHz Radio-frequency Ground Wave and Approximate Formulas for Computation," Brunavs, P., March 1977.

- [6] "Accuracy and Integrity Potential of Multichain Navigation", J. Cruz and R. Stoeckly, Illgen Simulation Technologies, Inc., Proc. International Loran Association 29th Annual Convention and Technical Symposium, November 2000.

- [7] "Covariance Analysis for On-the-fly ASF Calibration During Multichain Navigation", J. Cruz, Illgen Simulation Technologies, Inc., Proc. International Loran Association 29th Annual Convention and Technical Symposium, November 2000.

- [8] "WAAS Precision Approach Metrics Accuracy, Integrity, Continuity, and Availability," Stanford University WADGPS Laboratory, <http://waas.stanford.edu/metrics.html>.

BIOGRAPHIES

Jaime Cruz is a Principal Staff Engineer at ISTI. His experience includes navigation with Loran-C, the Global Positioning System, and the GPS Wide- and Local-Area Augmentation Systems, local and global gravity field modeling, satellite laser positioning of ground targets, satellite orbit estimation, and the development of an airborne gravity measuring system. Dr. Cruz received his Ph.D. in geodesy from The Ohio State University in 1985.

Robert Stoeckly has worked in radionavigation since 1997 as Senior Research Engineer at ISTI. His research includes experimental and theoretical work in Loran-C and simulations of the Wide-Area Augmentation System. Dr. Stoeckly previously conducted research in atmospheric physics. He received the Ph.D. in astrophysical sciences from Princeton University in 1964.

Robert Lilley leads Illgen Simulation's involvement in FAA's Systems Engineering Technical Assistance II program. He has been involved with validation and verification of GPS/WAAS system software, with the development of the WAAS Performance Assessment System and other navigation-related projects for the FAA, NASA and industry. He is also responsible for the company's Loran-C related

projects.

Dr. Lilley is Director Emeritus of the Avionics Engineering Center, Ohio University, earned his Ph.D. at Ohio University and is an instrument-rated commercial pilot. He was awarded the Medal of Merit by the International Loran Association for contributions to the Loran-C program. He is an ILA past-president and long-time member of the Board of Directors. Dr. Lilley was awarded the FAA's first Excellence in Aviation Award in 1997.

John Kirk is a Technical Manager at ISTI. His experience there includes analysis of corrections algorithms for wide- and local-area augmentations of the Global Positioning System and participating in the development of Loran-C navigation software. His previous experience includes development and use of satellite orbit management

software and managing operations of the GPS test constellation. Dr. Kirk received a Ph.D. in solar physics from The University of Michigan in 1966.

Steven Chavin is a senior member of the professional staff at ISTI supporting the ionospheric modeling effort of the WAAS system and, more recently, the Loran-C navigation effort. Prior to his work on WAAS he has about 12 years of ionospheric modeling experience for several Defense Nuclear Agency programs. Dr. Chavin has a Ph.D. in theoretical physics from the University of Illinois.

ACKNOWLEDGEMENT

The work described in this paper was sponsored by the "FAA AND-740 Loran-C Augmentation for GPS and GPS/WAAS" Program under Grant 99-G-038.

Table 1. Baseline LUPS configuration parameters.

Parameter and Value	Remark
chains = NEUS GLKS CEC (19 & 20 June, PC-104) NEUS SEUS CEC (21 June, PC-104) NEUS SEUS CEC (22 June 481234 – 482992 sec, DDC) NEUS SEUS GLKS (22 June 483056 – 491196 sec, DDC)	Loran-C chains tracked by the indicated receiver during the specified period.
cnot = $(0.108 \text{ m/km})^2$ corr1 = 200 km	Variance and correlation length of scale-factor error covariance function for the propagation delay spatial-error covariance model.
cnot_bar = $(0.108 \text{ m/km})^2$ corr1_bar = 1000 km	Variance and correlation length of scale-factor error covariance function for the propagation/emission delay temporal-variation covariance model.
sign02 = 2500 m^2	TOA noise variance at 0 dB SNR; TOA noise variance = sign02 x $10^{(-\text{SNR in dB} / 10)}$
emas = 30 m	Standard error of Master clocks with respect to UTC
esec = 6 m	Standard error in maintaining the controlling standard time difference (CSTD)
eothe = 110 m	Standard deviation of other error sources
ecd_tol = 10 μsec	ECD absolute-value threshold
sndb_min = -10 dB for PC-104 data; -15 dB for DDC data	SNR threshold
sig02 = 1.5	Reference variance

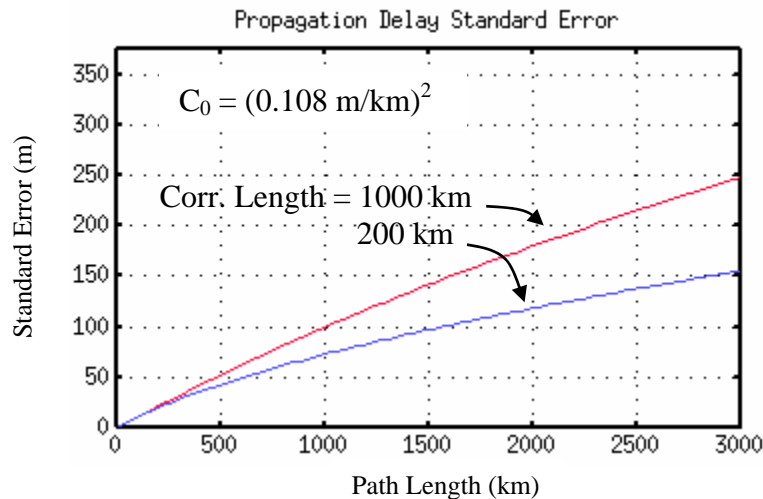


Figure 1. Propagation delay standard error implied by the scale-factor error covariance function of indicated variance and correlation length.

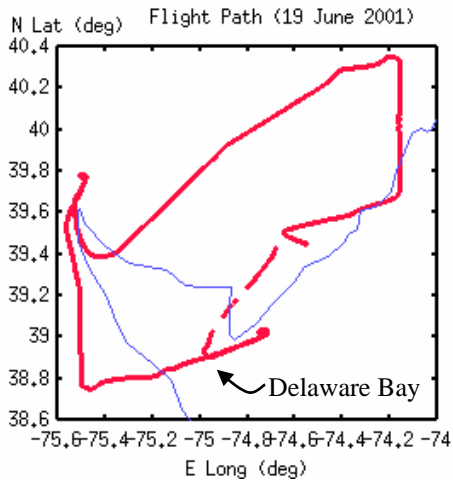


Figure 2. Flight path on 19 June 2001.

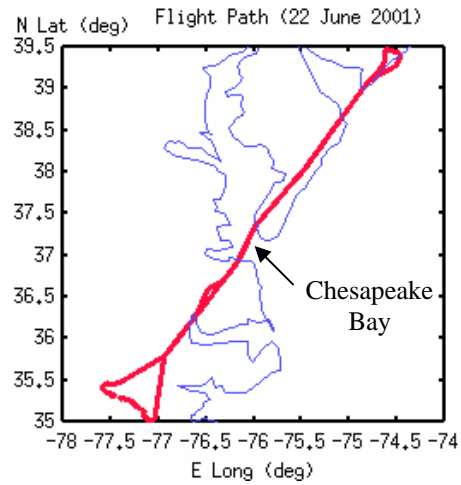


Figure 5. Flight path on 22 June 2001.

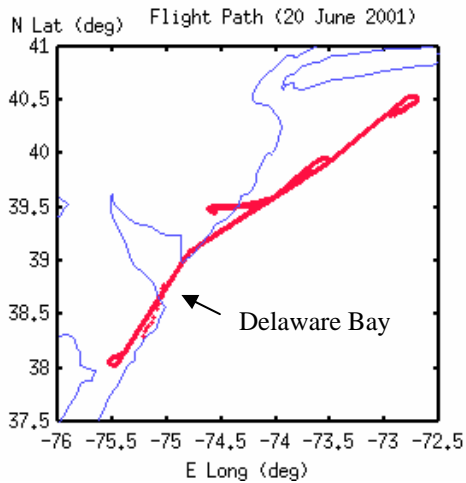


Figure 3. Flight path on 20 June 2001.

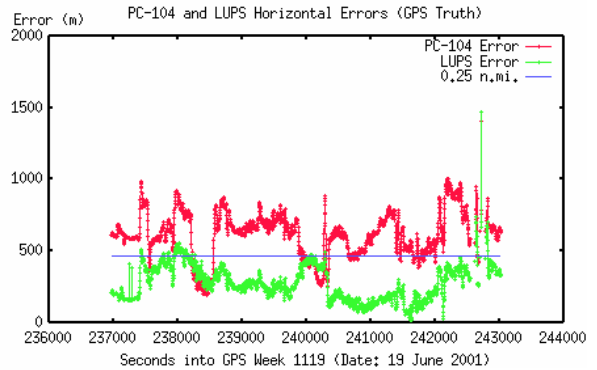


Figure 6. PC-104 and LUPS horizontal errors on 19 June 2001.

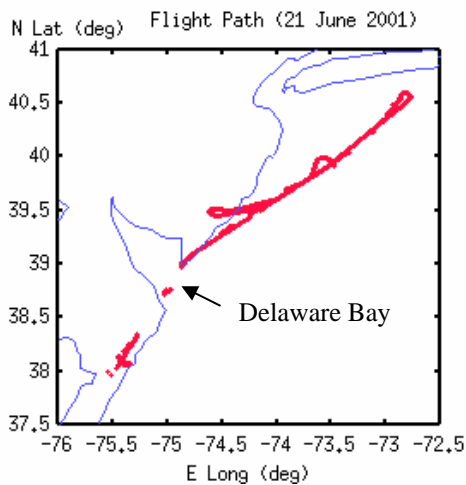


Figure 4. Flight path on 21 June 2001.

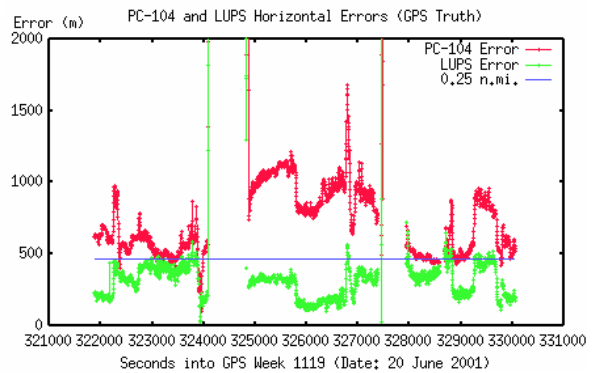


Figure 7. PC-104 and LUPS horizontal errors on 20 June 2001.

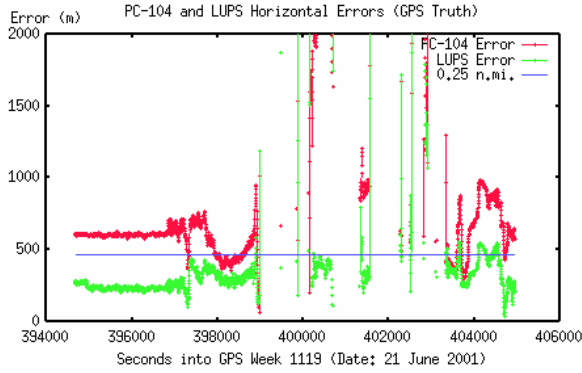


Figure 8. PC-104 and LUPS horizontal errors on 21 June 2001.

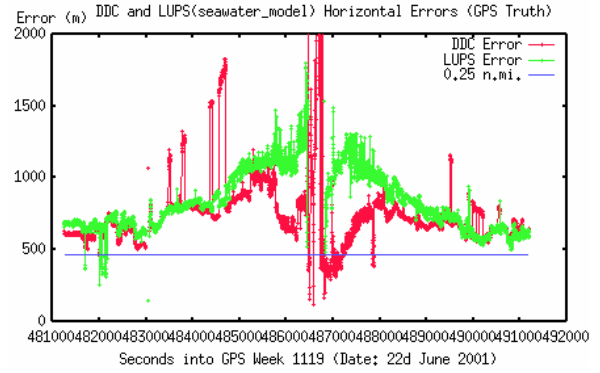


Figure 11. DDC and LUPS horizontal errors on 22 June 2001 when using the all-seawater propagation delay model in LUPS.

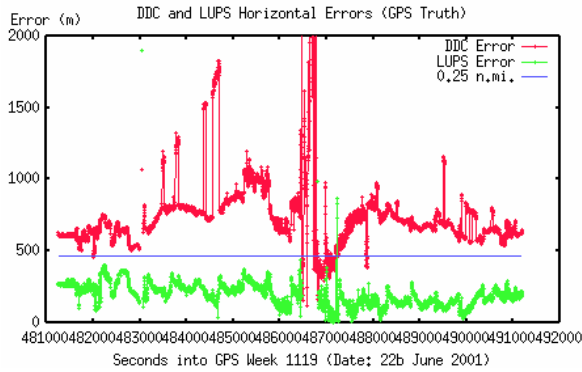


Figure 9. DDC and LUPS horizontal errors on 22 June 2001.

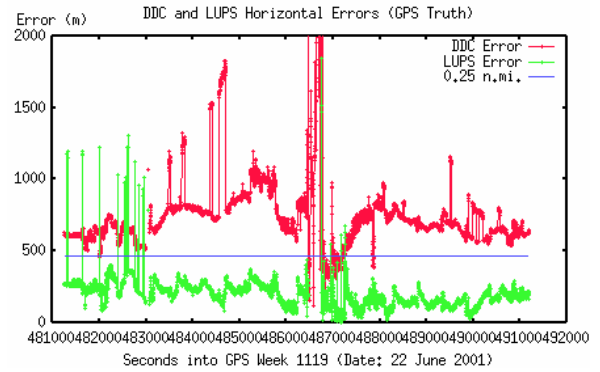


Figure 12. DDC and LUPS horizontal errors on 22 June 2001 when using an SNR threshold of -20 dB in LUPS.

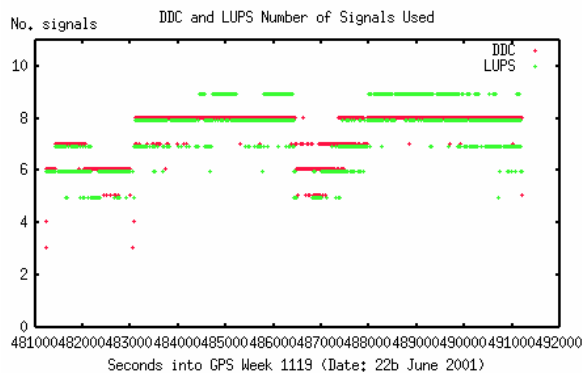


Figure 10. Number of signals used in the DDC and LUPS solutions on 22 June 2001.

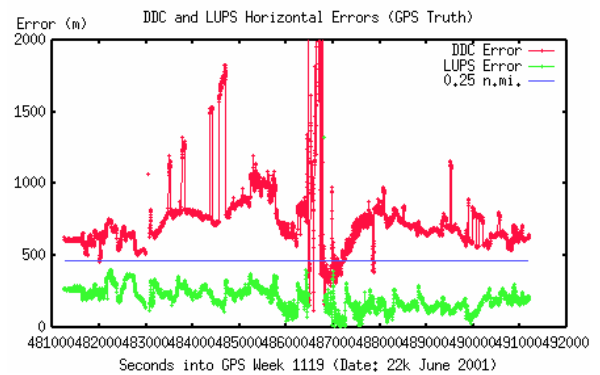


Figure 13. DDC and LUPS horizontal errors on 22 June 2001 for the case when LUPS used a standard deviation of 20 m at 0 dB SNR for the TOA-noise and 60 m for the "other" error sources.

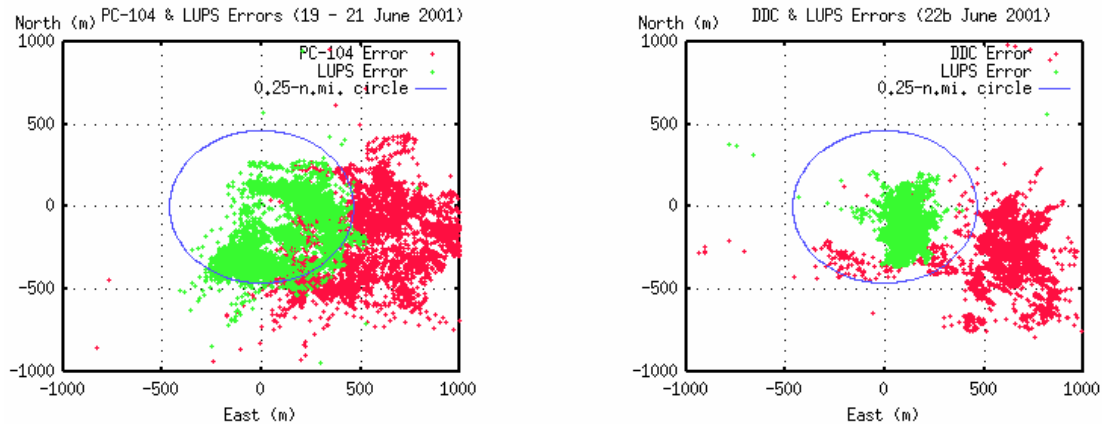


Figure 14. PC-104/DDC and LUPS East and North navigation errors with the 19 – 21 June 2001 PC-104 data (left) and 22 June 2001 DDC data (right).

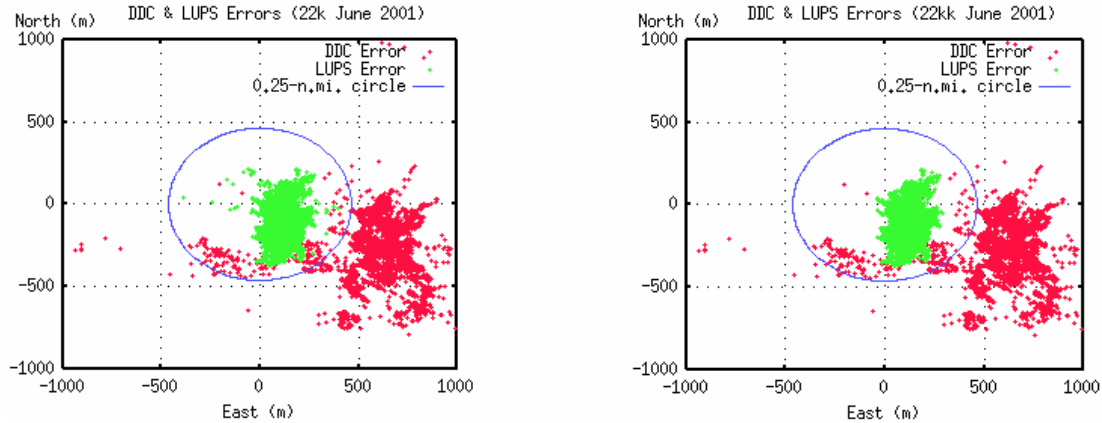


Figure 15. DDC and LUPS East and North errors with the 22 June 2001 DDC data, for the case when LUPS used a standard deviation of 20 m at 0 dB SNR for the TOA-noise and 60 m for other error sources, and including (left) or excluding (right) results between epochs 486400 – 487000 seconds UTC.

Table 2. Statistics of the LUPS horizontal navigation errors.

Navigation Solution	Original No. Samples	No. Samples Used	Average Error (m)	Std Dev Error (m)	95 % Error (m)	99.9 % Error (m)	Average No. Signals
Using the 19 – 21 June 2001 PC-104 receiver data (see Figure 14, left)	6207	5961 ⁽¹⁾	293	106	469	694	5.3
Using the 22 June 2001 DDC receiver data (see Figure 15, left)	4719	4719	204	85	322	399	7.6

⁽¹⁾ After excluding the three periods of abnormal receiver data (see Figure 18).

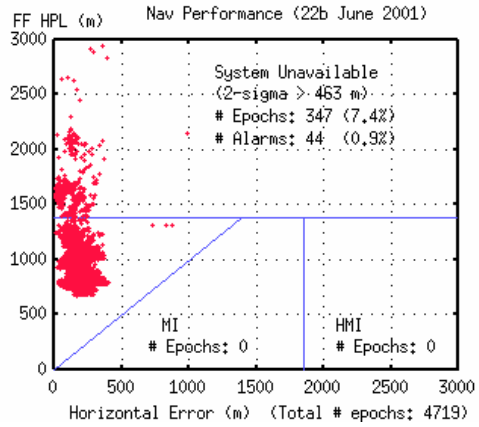
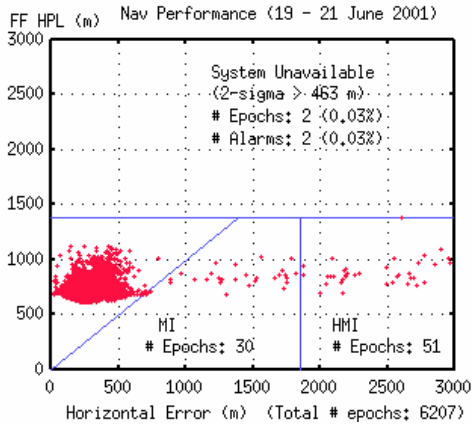


Figure 16. LUPS navigation performance with the 19 – 21 June 2001 PC-104 data (left) and 22 June 2001 DDC data (right).

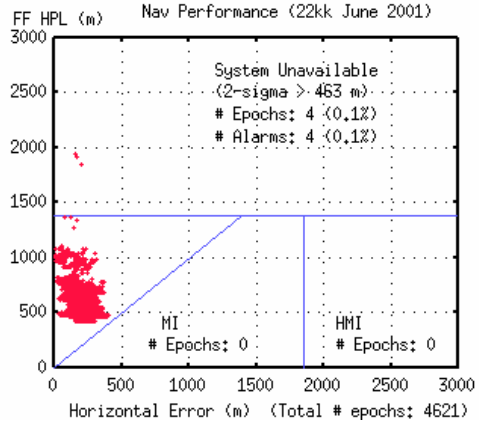
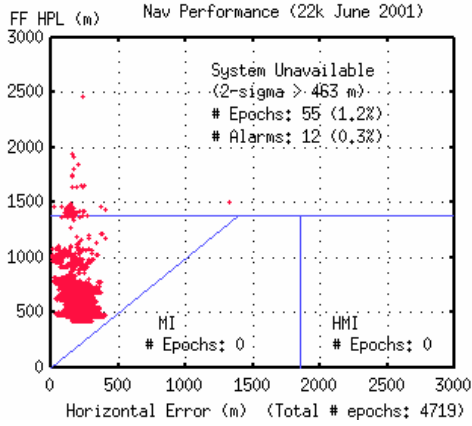


Figure 17. LUPS navigation performance with the 22 June 2001 DDC data for the case when LUPS used a standard deviation of 20 m at 0 dB SNR for the TOA-noise and 60 m for other error sources and including (left) or excluding (right) results between epochs 486400 – 487000 seconds UTC.

Figure 18. LUPS navigation performance using the 19 – 21 June 2001 PC-104 data, with the following epochs of abnormal receiver data excluded from the plot: 324072 – 324870, 327450 – 327930, and 398976 – 403221 seconds UTC.

